Real-Time Scheduling for Cognitive Radio Networks

Shabnam Sodagari, *Senior Member, IEEE*

***Abstract*—Real-time scheduling protocols for cognitive radio (CR) networks that can be implemented in the spectrum manager of IEEE 802.22 are proposed. The protocols take into consideration the inherent uncertainties in CR networks that are caused by the unknown future primary user channel usage and the dynamic channel allocation demands of the CR users in each time slot. Scheduling is performed at the beginning of each time slot. The proposed mean throughput maximization (MTM) scheduling protocol schedules the CRs available in the current time slot considering past channel allocations and possible future demands without introducing the delay of waiting for future CR resource demands to be revealed. A variation of the MTM called throughput loss minimization (TLM) is introduced to further reduce the delay in MTM scheduling. The upper bound on the throughput loss and the relation of TLM to MTM in terms of computational complexity and approximation ratio are analyzed. In addition, Markov chance decision processes are used for CR real-time scheduling. Tradeoffs in the upper bound of the throughput loss allow the cognitive base station to enhance the sum throughput of the CR network to maintain both scheduling time and throughput loss below a desired level.**

***Index Terms*—Cognitive radio (CR), dynamic spectrum access, IEEE 802.22 standard, medium access control (MAC).**

I. Introduction

COGNITIVE radio networks (CRNs) opportunistically take advantage of white spaces of primary users (PUs). A white space is an unused radio resource that can depend on time, frequency, and geographical location, and its utilization should not cause interference to PUs [1]. Due to the opportunistic use of spectrum, CRNs are unpredictable by nature. More precisely, in addition to the unknown traffic arrival times and number of packets, which are common to all communication networks, the future activities of the PUs are also unknown. Therefore, in order for the decision making of the cellular cognitive base station (CBS) to be efficient for CRNs, the future activities of the PUs should be taken into account. In other words, this is not a problem with fully known cognitive radio (CR) users resource needs over the time horizon. At any time, a PU may suddenly become active in a band, resulting in the CR using that band to refer to the CBS for a new resource. The contribution of this paper is the novel decision making of the CBS. This paper is the first work to use Markov chance decision processes for real-time scheduling in CRNs and to study throughput upper bounds of sampling for real-time scheduling in CRNs.

Manuscript received November 8, 2016; revised May 12, 2017, September 12, 2017, and November 3, 2017; accepted November 4, 2017. Date of publication November 23, 2017; date of current version August 23, 2018. *(Corresponding author: Shabnam Sodagari.)*

The author is with the Department of Electrical Engineering, California State University, Long Beach, CA 90840 USA (e-mail: shabnam@ieee.org).

Digital Object Identifier 10.1109/JSYST.2017.2771328

The medium access control (MAC) scheduling proposed in this paper aims to maximize the aggregate throughput while implementing fairness among CRs contending for channels. Hence, the main contributions of this paper are targeted toward addressing the following issues.

1) Throughput-optimized MAC scheduling schemes in CRNs that take into account the unpredictability of CRNs.
2) Addressing the short-lived nature of PU white spaces by real-time decision making in CRNs while yielding optimal throughput without having to wait to collect all the data.
3) Introducing the mean throughput maximization (MTM) scheduling scheme.
4) Enhancing the convergence time of MTM by proposing throughput loss minimization (TLM) scheduling.
5) Using Markov chance decision processes for CR scheduling.
6) Deriving bounds on the throughput loss and computational complexity.

The rest of this paper is organized as follows. Section II provides a literature survey that summarizes the state of the art in this field. In Section III, the structure of the problem and the proposed cognitive scheduling schemes are elaborated. Section IV presents the throughput bounds of the proposed method. Sections V and VI apply Markov chance decision processes to real-time CR scheduling. Section VII analyzes the computational complexity of the proposed CR scheduling methods. Numerical results are presented in Section VIII. Finally, Section IX concludes the paper.

Table I contains the notation and abbreviations used throughout this paper.

II. Background

Chen *et al.* [2] investigate network formation for spectrum management in CR mesh networks. They propose a cluster-based approach for neighbor discovery and control when there is no global control channel available. They optimize the cluster configuration considering the network topology. Furthermore, Jia *et al.* [3] take hardware constraints into account for spectrum management in *ad hoc* CRNs. They formulate the sensing and transmission-constrained problem as an optimal stopping problem. In their decentralized MAC, they optimize the sensing decision in a sequence of sensing processes. In contrast, this paper proposes a centralized MAC in which the CBS performs the task of sensing. Additionally, Tumuluru *et al.* [4] apply Markov chain and queuing theory to centralized MAC scheduling to estimate the expected number of packets to be transmitted by a CR over each PU channel within a frame. In another work, Tumuluru *et al.* [5] divide CR traffic into high- and low-priority

TABLE I
NOTATION AND ABBREVIATION

PU	Primary user
CR	Cognitive radio
CRN	Cognitive radio network
MAC	Medium access control
WRAN	Wireless regional area network
CBS	Cognitive base station
MTM	Mean throughput maximization
TLM	Throughput loss minimization
NRT	Non-real-time
MCDP	Markov chance decision process
E[.]	Expected value
$\mathcal{T}$	End time slot in horizon
$\mathscr{T} = \{1, \ldots, t, \ldots, \mathcal{T}\}$	Set containing all time slots
$t \in \mathscr{T}$	Current time slot t
D_t	Set of channel scheduling demands by CRs for time slot t
$\omega_{t+1,\ldots,\mathcal{T}}$	Samples of probability distribution representing CR demands in future time slots
$k_{\max}$	Maximum time slots the channel is allocated to a single CR
$d : \omega_{t+1,\ldots,\mathcal{T}}$	Concatenation of current channel demand d and samples representing future channel demands
a_t	Scheduling decision made by CBS at time t
$\mathbf{a}_{t-1}$	Past scheduling decisions made by CBS at times $1, \ldots, t-1$
$\mathscr{R}(\mathbf{a}_{t-1}, d)$	Rate or throughput obtained by scheduling CR d at time slot t, given past decisions $\mathbf{a}_{t-1}$
d_{MTM}	CR scheduled by CBS using MTM scheduling
$\mathbb{P}(.)$	Probability of a random variable
m	Number of samples
σ_t^2	Variance of throughput loss at each time slot
L_t	Expected value of throughput loss at each time slot
$\mathbb{R}$	Set of real numbers
s_{t+1}^{MCDP}	Next state of CRN white space usage determined by MTM MCDP scheduling
$\mathscr{C}$	MCDP chain of alternating states and observations
ξ_t	Markov chain representing PU activities
i_t	Input observation of the CRN at time t imposed by the PU activity
$\mathcal{L}_{t1}$	Throughput loss per time slot of MCDP CRN scheduling due to (34)
$\mathcal{L}_{t2}$	Throughput loss per time slot of MCDP CRN scheduling due to empirical averaging
$\mathcal{L}_t$	Expected value of per time slot total throughput loss of MCDP CRN scheduling

classes. They study the effects of different centralized and distributed schemes on prioritized traffic with spectrum handoff, which occurs upon the return of a PU to the channel. To this end, they use continuous-time Markov chains. In addition, the energy efficiency of CRNs, heterogeneous networks, and sensor networks using big data is addressed in [6]–[9].

As relates to PU activity models, Xing *et al.* [10] summarize spectrum prediction methods in CRNs. They present an overview of prediction techniques, such as the hidden Markov model, multilayer perception neural networks, Bayesian inference, moving average, autoregressive models, and static neighbor graphs applied to CRNs. Moreover, Chen *et al.* [11] conduct a survey of spectrum occupancy models from measurements in different geographical regions, up to 2013. The measurements extract some statistics, such as the duty cycle, cumulative distribution function, and probability density function. Nevertheless, as mentioned in [12], many spectrum occupancy studies reported in the literature are based on measurements with a single device at a fixed location. In another survey of PU activity models [13], PU spectrum utilization is classified via the Markov process, queuing theory, time series, on/off, Bayesian, and event-based random walk, among other models. Also, the Bernoulli model for both PU and CR activities is considered in [14]–[16]. Specifically, Ganti *et al.* [14] consider arrival and channel states as Bernoulli processes, and Banaei *et al.* [15] model a user's active or inactive status over a channel as a Bernoulli random variable. Additionally, Gambini *et al.* [16], [17] consider the packet arrival processes for CRs and PUs at each node as independent Bernoulli processes. In this paper, a generic model using Markov chance decision processes, which encompasses both the PU activity and the resulting optimal CRN schedules, is presented. In other words, the PU activity is modeled as a Markov chain that affects the CRN. However, the CRN decision based on the PU activity is modeled as a Markov chance decision process, rather than a Markov decision process.

Hsu *et al.* [18] propose a carrier sense multiple access (CSMA)-/CA-based cognitive MAC using statistical channel allocation. Their decentralized scheme uses statistics of spectrum usage for decision making on channel access. Transmission parameters are negotiated using a control channel between the sender and the receiver for each transmission. Thilina *et al.* [19] consider the problem of common control channel for centralized MAC in CRNs. They propose a dynamic common control channel, in contrast to the traditional dedicated control channel, for MAC protocols. They use a support vector machines learning mechanism to implement a dynamic common control channel. In their scheme, CRs who participate in the dynamic common control channel selection process are scheduled to transmit their traffic while other CRs have to contend for access to the channels.

Contrary to previous works, including the ones mentioned above, this paper takes a proactive rather than reactive approach

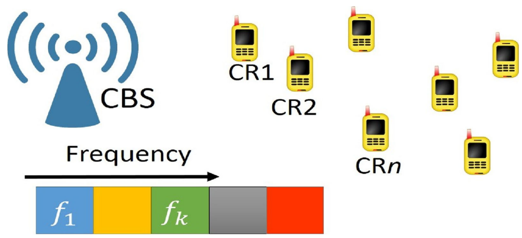

Fig. 1. CBS channel scheduling considering CRs demands.

to the design of MAC in CRNs. The protocols in this paper can be used to enhance the performance of IEEE 802.22 wireless regional area networks (WRANs). In such networks, CRs use bandwidth request slots within an IEEE 802.22 frame to let the CBS know about their dynamic need for resources. Without loss of generality, the CBS can be implemented in the cloud.

III. System Model and Proposed Cognitive Scheduling Schemes

Similar to the IEEE 802.22 standard, which is a centralized scheme for WRANs, using white spaces [20], a CBS performs the task of channel scheduling. As shown in Fig. 1, the CBS schedules the idle channels of PUs to CRs with traffic to transmit.

The model considers time frames of duration T seconds, e.g., similar to the IEEE 802.22 frame structure. The first portion of a time frame is dedicated to scheduling, and the remaining part is used for CRs transmission. At the beginning of each time frame, the CBS considers the requests of the CRs and decides whether a CR can be scheduled to transmit in the current time frame.

Since the method of this paper is based on the interweave CRN paradigm, which involves spectrum sensing to detect white spaces, interference to the PU can be avoided. This is different from underlay (e.g.,[21] and [22]) or overlay CR schemes [23] that might cause some level of interference to the PU. Specifically, in underlay and overlay CRNs, the CRs or secondary users are allowed to transmit at the same time and over the same band as the PU, conditioned on keeping the interference to the PU below a certain threshold or helping to relay the PU message. However, in interweave CRNs, which are based on spectrum sensing, transmission only happens when the PU is not on the band to avoid any interference to the PU. Specially, if the CRN is full duplex [24], i.e., can sense and transmit at the same time, it can immediately stop transmitting upon detection of the PU to prevent interference.

Here, the CBS scheduling decision is based upon higher overall throughput, considering the unknown future of the CRN. Another objective is to implement fairness among CRs. To this end, the proposed cognitive scheduling equips a CBS with two modules: one for optimizing the CRN throughput and the other for generating scenarios that may occur in future time slots due to unknown future PU and CR activities. In this regard, the CBS generates samples of future requests [25] and associated throughputs. To implement fairness, each CR can receive the band a maximum of $k_{\max}$ times over all time slots in the horizon. Sampling enables the CBS to improve the overall CRN throughput over all time slots. Considering the fairness constraint, instead of hastily allocating current CRs $k_{\max}$ times, by sampling the future, the CBS does not lose future schedules of higher throughput.

Formally, consider a set of CRs $\mathscr{N} = \{1, 2, \ldots, N\}$. For $n \in \mathscr{N}$, denote a CR by CR n. At the beginning of each time frame t, the CBS receives a set of scheduling demands from the CRs. The set of all scheduling demands for the time horizon $\{1, 2, \ldots, t\}$ is $\{D_1, D_2, \ldots, D_t\}$. Here, D_t is the set of CRs that announce their need for a resource in time frame t. For example, $D_2 = \{\text{CR}_2, \text{CR}_5, \text{CR}_7\}$ means that at the beginning of the second time frame, the CBS has to decide which of CR3, CR5, or CR7 to schedule. The objective of the CBS at time t is to maximize the overall CRN throughput over the past, present, and future time horizon $\mathscr{T} = \{1, 2, \ldots, t, \ldots, \mathcal{T}\}$. However, future demands $\{D_{t+1}, \ldots, D_{\mathcal{T}}\}$ are unknown at the present time t. Past scheduling decisions have been made at time slots $1, \ldots, t-1$. Due to immediate needs of CRs traffic, the CBS cannot wait to collect all demands up to time $\mathcal{T}$ to make a decision. In other words, the CBS has to provide a real-time multiple-access scheme. In this regard, this paper proposes that the CBS generates future demands by sampling the distribution of demands and concatenating them alongside the current demand at time t to determine which current demand maximizes the overall throughput and should be scheduled at this time.

A conventional optimization allocates resources to the CR that has the maximum throughput at the current time without considering it within the context of future resource allocation requests. The CBS considers each CR along with past allocations, denoted by $\mathbf{a}_{t-1}$, and possible future requests, related to time slots $t+1, \ldots, \mathcal{T}$ and denoted by $\omega_{t+1,\ldots,\mathcal{T}}$. Possible future requests are obtained by sampling. The CBS then optimizes the throughput of each scenario and allocates the resource to the CR that yields the highest throughput in the present and future, considering the fairness constraint explained above.

Information about the PU channel status and the CR channel demands is not available in advance but is revealed incrementally. The optimal strategy in cognitive multiple access is not simply selecting the CR with the highest immediate signal-to-noise ratio (SNR) at time t but considering every CR demand in the context of past schedules and future demands. For example, consider CR n that has been scheduled $k_{\max} - 1$ time slots out of the past $t-1$ time slots. In time slot t, the same CR n is demanding the channel and has the highest SNR among all CRs over that band. If the sampling shows that the same CR n will have even better SNR in future time slots, the CBS does not schedule CR n at time t, but postpones its scheduling to the future to maximize the sum throughput over all time slots in the horizon. More numbers of sample sets lead to more accurate scheduling decision by the CBS. In other words, if the CBS can take several sets of samples, representing time slots $t+1, \ldots, \mathcal{T}$, it can make a more informed decision by averaging. However, PU white spaces are short lived, and the coordination time in CRNs is limited. Accordingly, the CBS can take only a few sets of samples. In spite of this limitation, this paper shows how to obtain optimal CRN schedules.

Formally, the CBS considers a time horizon $\mathcal{T}$ and a number of channel demands. Each CR d, available at time slot t, has an SNR proportional to the rate or throughput $\mathscr{R}$ over the band. The goal is to find a constrained solution that maximizes $\sum_{t=1}^{\mathcal{T}} \mathscr{R}(a_t)$. Here, a_t denotes the scheduling decision of the CBS at time t. In the proposed MTM scheduling scheme, the CBS evaluates each CR's present demand (SNR) against multiple sets of samples representing future demands and their rates or SNRs. This may be achieved by letting the CRs conduct a quick channel sounding experiment at the beginning of each time slot to get a sense of their approximate capacity over the channel.

The evaluation of a CR resource demand d is incrementally updated by considering each set of samples. Finally, at the end of the limited decision time, the CR with the highest evaluation score receives the band in time slot t. The throughput loss of this method depends on the number of sample sets that are permitted during the short decision time at the beginning of each frame. Since the CBS compares every CR demand against sets of samples, the total time to make the decision is divided among the number of CRs currently demanding the channels. Accordingly, when the scheduling time is short, each current CR demand is considered within the context of a smaller number of sample sets. Therefore, some overall throughput loss is inevitable in MTM MAC scheduling, in contrast to the non-real-time (NRT) delayed scheduling. Nevertheless, this paper shows that this throughput loss is upper bounded and the upper bound is achievable by increasing the number of samples.

To compromise between the speed of the scheduling decision and accuracy, in terms of throughput loss, the CBS can use TLM MAC. When using TLM scheduling, the CBS evaluates each available channel demand for every sample with an upper bound for throughput loss. TLM quickly estimates the throughput loss of a sample set of CR demands, i.e., the difference between the throughput and an upper bound for performance. At the end of the scheduling time, the CR with the least total difference over all generated samples for all rounds receives the channel. MTM medium access scheduling requires more time than TLM. The TLM scheme is useful when CBS is handling a large number of CR demands or when the number of samples is small. This is due to the fact that in TLM scheduling, in contrast to MTM, the CBS does not partition available samples among CR demands. Hence, TLM is able to consider more samples in the allowed scheduling time because it does not distribute the optimizations among CR demands. This implies that for the same available decision time for the CBS, the number of sample sets that can be considered in TLM is equal to the number of sample sets that can be considered in MTM multiplied by the number of available CRs in the current time slot.

Denoting the total number of CRs resource allocation demands by $|D|$, TLM is $|D|$ times faster than MTM because TLM does not consider every CR demand versus every set of samples, whereas MTM considers each CR demand versus every sample set. Deeper insights into MTM and TLM are presented in the following sections. In particular, MTM and TLM are studied in the context of a Markov Chance Decision Process (MCDP) in Sections V and VI. In Section V, similarities and differences between Markov decision processes and MCDPs are presented. This is a general framework to optimize CRN scheduling, by considering the effects of PU activity on the CRN as an exogenous parameter that leads the CBS to change states. As shown in Fig. 2, the PU activities are modeled as a Markov chain ξ_t that evolves independently from the CRN but affects the CRN white space usage decisions. At each time t, the CRN is in state s_t and the input observation i_t, which is a realization of ξ_t, is imposed upon it because the PU has priority for channel usage. The input i_t causes transition to a new state s_{t+1}. In Section V, optimal scheduling strategies for the CBS are investigated using the notion of an MCDP chain, which is a sequence of alternating states and observations.

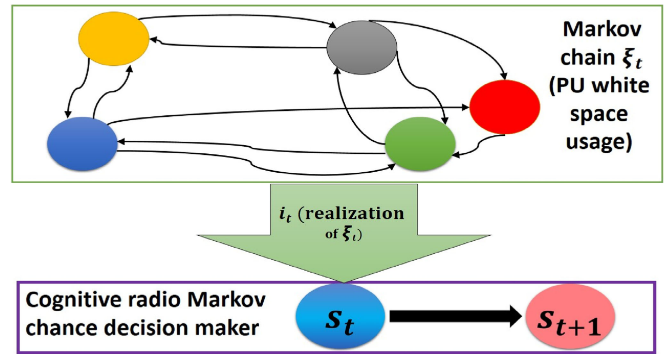

Fig. 2. CR real-time scheduling using Markov chance decision processes.

Section IV presents an upper bound on the performance of the proposed scheduling methods.

IV. Throughput Bound of the Proposed Scheduling

The goal of this analysis is to determine the expected loss of the MTM real-time multiple access scheme. Specifically, MTM is compared with the ideal case when the CBS has noncausal knowledge of the SNRs of all CRs over the channels in all future time slots. This section answers the question of how many samples are required to obtain a solution that closely approximates the most optimal solution. Particularly, to benchmark the solution, the average difference between the real-time MTM medium access scheme and the NRT case, where the CBS waits until the final time slot to collect all the information and then schedules channels to CRs in each time slot, is determined. An upper bound for the losses in throughput in each time slot is presented. The expected loss of the proposed MTM scheduling is the sum of the throughput losses in each time slot.

The CBS converts the real-time scheduling problem into an NRT optimization problem by replacing future CR demands with samples from a probability density function. The CBS then solves this optimization to obtain $\mathscr{R}_{\mathrm{NRT}}$, which is the throughput of the NRT channel scheduling, i.e., the case where the CBS waits until the final time slot for all CR demands to be revealed and then retroactively schedules for each time slot. $\omega_{\mathscr{T}}$ is drawn from the underlying distribution that determines the CR demands and their SNRs.

In each time slot $t \in \mathscr{T}$, there is a channel demand by a CR that is selected to maximize the expected sum throughput over all time slots $\{1,\ldots,\mathcal{T}\}$ for realizations D_t of ω_t and the vector of past channel allocations $\mathbf{a}_{t-1}$. Channel allocation to a single CR is limited to $k_{\max}$ slots during all time slots in $\mathscr{T}=1,\ldots,\mathcal{T}$. Note that

$$\underset{\omega_{t,\ldots,\mathcal{T}}|\omega_{1,\ldots,t-1}}{\mathrm{E}}\left[\mathscr{R}_{\mathrm{NRT}}\left(\mathbf{a}_{t-1},\omega_{1,\ldots\mathcal{T}}\right)\right] = \underset{\omega_t|\omega_{1,\ldots,t-1}}{\mathrm{E}}\left[\max_{d_t}\left(\underset{\omega_{t+1,\ldots,\mathcal{T}}|\omega_{1,\ldots,t}}{\mathrm{E}}\left(\mathscr{R}_{\mathrm{NRT}}(\mathbf{a}_t,\omega_{1,\ldots\mathcal{T}})\right) + \mathscr{R}\left(\mathbf{a}_{t-1},d_t\right)\right)\right]. \quad (1)$$

for all times $t\in\mathscr{T}$. Here, $\mathscr{R}_{\mathrm{NRT}}\left(\mathbf{a}_{t-1},\omega_{t\ldots\mathcal{T}}\right)$ denotes the throughput obtained by the NRT scheduling with knowledge of past allocations $\mathbf{a}_{t-1}$ along with CR demands for the present and future time slots. d_t is the variable for CR demand at time t, and E[.] denotes the expected value. Channel access depends on samples ω, which represent future demands. When the number of samples representing the future grows, this medium access protocol approaches the most optimal solution. This section determines how many samples are needed for the solution to be as optimal as the NRT, i.e., the delayed case until the end of the time horizon $\mathcal{T}$, when the actual CR demands and SNRs for all time slots (that are considered future for the real-time scheduling) have been revealed to the CBS.

The CBS should select the CR at time t with demand d^* such that

$$d^*=\arg\max_{d}\mathrm{E}[\mathscr{R}_{\mathrm{NRT}}(\mathbf{a}_{t-1}:d\in D_t:\omega_{t+1,\ldots,\mathcal{T}})] \quad (2)$$

subject to scheduling d_t^* for less than or equal to $k_{\max}$ time slots in a total of $\mathcal{T}$ slots. The average sum throughput for the above is

$$\mathrm{E}\left[\mathscr{R}_{\mathrm{NRT}}\left(\mathbf{a}_{t-1}:d^*\in D_t:\omega_{t+1,\ldots,\mathcal{T}}\right)\right]. \quad (3)$$

Nevertheless, in real-time MTM scheduling, the CBS has only a limited time to make a decision. Accordingly, it has a limited set of samples at hand. Practically, the CBS may not be able to identify the actual best CR demand d^*. Instead, it may select a CR demand d (not being allocated more than $k_{\max}$ times in previous time slots) with expected throughput

$$\mathrm{E}\left[\mathscr{R}_{\mathrm{NRT}}\left(\mathbf{a}_{t-1}:d\in D_t:\omega_{t+1,\ldots,\mathcal{T}}\right)\right]. \quad (4)$$

Denote the expected value of throughput loss at each time slot t by $L_t\left(d,\mathbf{a}_{t-1},\omega_{1,\ldots,t}\right)$. The throughput loss given in (5) is the difference in throughput obtained by scheduling the best possible CR d^* with that of CR d returned by MTM

$$\begin{aligned}L_t\left(d,\mathbf{a}_{t-1},\omega_{1,\ldots,t}\right) &= \max_{d^*}\left(\mathscr{R}\left(\mathbf{a}_{t-1},d^*\right)+\underset{\omega_{t+1,\ldots,\mathcal{T}}}{\mathrm{E}}[\mathscr{R}_{\mathrm{NRT}}(\mathbf{a}_{t-1},d^*,\omega_{1,\ldots,\mathcal{T}})]\right)\\ &\quad -\left(\mathscr{R}(\mathbf{a}_{t-1},d)+\underset{\omega_{t+1,\ldots,\mathcal{T}}}{\mathrm{E}}[\mathscr{R}_{\mathrm{NRT}}(\mathbf{a}_{t-1}:d,\omega_{1,\ldots,\mathcal{T}})]\right). \quad (5)\end{aligned}$$

It can be shown that the expected value of the throughput loss of the real-time MTM scheduling method is the sum of the throughput losses over all time slots, as shown in (6).

$$\sum_{t\in\mathscr{T}}\underset{\omega_{1\ldots,t}}{\mathrm{E}}\left[L_t\left(d_{\mathrm{MTM}}\left(\mathbf{a}_{t-1},\omega_{1,\ldots,t}\right),\mathbf{a}_{t-1},\omega_{1,\ldots,t}\right)\right] = \underset{\omega_{1,\ldots,\mathcal{T}}}{\mathrm{E}}\left[\mathscr{R}_{\mathrm{NRT}}\left(\omega_{1,\ldots,\mathcal{T}}\right)-\mathscr{R}_{\mathrm{MTM}}\left(\omega_{1,\ldots,\mathcal{T}}\right)\right]. \quad (6)$$

Equation (6) indicates that to derive an upper bound on the sum throughput loss over all time slots, it suffices to derive an upper bound on the throughput loss in each time slot t and then add the results for all time slots $t\in\mathscr{T}$ [26]. Note that the MTM is based on scheduling a CR that maximizes the mean throughput. In other words, for each CR demand d, the MTM calculates the empirical average obtained by sampling the probability distribution as

$$\begin{aligned}\underset{\omega_{t+1,\ldots,\mathcal{T}}|\omega_{1,\ldots,t}}{\mathrm{E}}&\left[\mathscr{R}_{\mathrm{NRT}}\left(\mathbf{a}_{t-1}:d,\omega_{1,\ldots,\mathcal{T}}\right)\right]\\ &\approx\frac{1}{m}\sum_{k=1}^{m}\mathscr{R}_{\mathrm{NRT}}\left(\mathbf{a}_{t-1}:d,\omega_{1,\ldots,t}:\omega_{t+1\ldots\mathcal{T}}^{k}\right)\\ &=Y\left(\mathbf{a}_{t-1}:d,\omega_{1,\ldots,t}\right) \quad (7)\end{aligned}$$

where $\omega_{t+1\ldots\mathcal{T}}^{k}$ denotes the kth set of samples from the probability distribution [26] representing the CRs demands for future time slots $t+1,\ldots,\mathcal{T}$. The CR selected by MTM MAC is

$$d_{\mathrm{MTM}}\left(\mathbf{a}_{t-1},\omega_{1,\ldots,t}\right)=\max\left(\mathscr{R}\left(\mathbf{a}_{t-1},d\right)\right)+Y\left(\mathbf{a}_{t-1}:d,\omega_{1,\ldots,t}\right) \quad (8)$$

and the solution to the delayed NRT method is

$$d^*=\max_{d}\left(\mathscr{R}\left(\mathbf{a}_{t-1},d\right)+\underset{\omega_{t+1,\ldots,\mathcal{T}}|\omega_{1,\ldots,t}}{\mathrm{E}}[\mathscr{R}_{\mathrm{NRT}}(\mathbf{a}_{t-1}:d,\omega_{1,\ldots,\mathcal{T}})]\right). \quad (9)$$

Note that for a given sample set, TLM computes only the optimal solution, whereas MTM also evaluates nonoptimal solutions. In other words, TLM only approximates the nonoptimal solutions, rather than rigorously calculating them, as in MTM [27]. To this end, TLM MAC aims to minimize the following difference:

$$U-\mathscr{R}(\mathbf{a}_{t-1},\omega_{t,\ldots,\mathcal{T}}) \quad (10)$$

where U can be a desired upper bound for throughput.

When the CBS uses MTM scheduling, it approximates the expected value by averaging the solutions obtained from the limited sample sets, allowed during the short CRN scheduling time. This means, in general, that the CBS schedules CR d_{MTM} instead of d^*. Therefore

$$\mathscr{R}\left(\mathbf{a}_{t-1},d_{\mathrm{MTM}}\right)+Y\left(\mathbf{a}_{t-1}:d_{\mathrm{MTM}},\omega_{1,\ldots,t}\right)\geq\mathscr{R}\left(\mathbf{a}_{t-1},d^*\right)+Y\left(\mathbf{a}_{t-1}:d^*,\omega_{1,\ldots,t}\right). \quad (11)$$

Following the procedure presented in [26], by rearranging (11), and using the definition of $L_t\left(d_{\mathrm{MTM}},\mathbf{a}_{t-1},\omega_{1,\ldots,t}\right)$ in (5), the following inequality for throughput loss at each time slot is obtained

$$\begin{aligned} &L_t\left(d_{\mathrm{MTM}}, \mathbf{a}_{t-1}, \omega_{1,\ldots,t}\right) \\ &\quad \leq Y\left(\mathbf{a}_{t-1} : d_{\mathrm{MTM}}, \omega_{1,\ldots,t}\right) - Y\left(\mathbf{a}_{t-1} : d^*, \omega_{1,\ldots,t}\right) \\ &\qquad - \underset{\omega_{t+1,\ldots,\mathcal{T}}|\omega_{1,\ldots,t}}{\mathrm{E}} \left[\mathscr{R}(\mathbf{a}_{t-1} : d_{\mathrm{MTM}}, \omega_{1,\ldots,\mathcal{T}})\right] \\ &\qquad + \underset{\omega_{t+1,\ldots,\mathcal{T}}|\omega_{1,\ldots,t}}{\mathrm{E}} \left[\mathscr{R}_{\mathrm{NRT}}\left(\mathbf{a}_{t-1} : d^*, \omega_{1,\ldots,\mathcal{T}}\right)\right]. \end{aligned} \tag{12}$$

Using the right-hand side of the inequality in (12), define

$$\begin{aligned} Z_{t,d} &= Y\left(\mathbf{a}_{t-1} : d, \omega_{1,\ldots,t}\right) - Y\left(\mathbf{a}_{t-1} : d^*, \omega_{1,\ldots,t}\right) \\ &\quad - \underset{\omega_{t+1,\ldots,\mathcal{T}}|\omega_{1,\ldots,t}}{\mathrm{E}} \left[\mathscr{R}\left(\mathbf{a}_{t-1} : d, \omega_{1,\ldots,\mathcal{T}}\right)\right] \\ &\quad + \underset{\omega_{t+1,\ldots,\mathcal{T}}|\omega_{1,\ldots,t}}{\mathrm{E}} \left[\mathscr{R}_{\mathrm{NRT}}\left(\mathbf{a}_{t-1} : d^*, \omega_{1,\ldots,\mathcal{T}}\right)\right]. \end{aligned} \tag{13}$$

In (13), the term

$$Y\left(\mathbf{a}_{t-1} : d, \omega_{1,\ldots,t}\right) - Y\left(\mathbf{a}_{t-1} : d^*, \omega_{1,\ldots,t}\right) \tag{14}$$

is the sum of m independent identically distributed (i.i.d.) random variables. Here, m is the number of samples per time slot. Denote the variance of each i.i.d. random variable, associated with throughput loss in each time slot, by σ_t^2. By the central limit theorem, $\frac{\sqrt{m}Z_{t,d}}{\sigma_t}$ is a standard normal random variable. The above analysis [26] results in finding the expected value of the throughput loss of MTM MAC in each time slot. By (12)

$$\mathbb{P}\left(d_{\mathrm{MTM}}|\omega_{1,\ldots,t}\right) \leq \mathbb{P}\left(L_t\left(d, \mathbf{a}_{t-1}, \omega_{1,\ldots,t}\right) \leq Z_{t,d}|\omega_{1,\ldots,t}\right) \tag{15}$$

where $\mathbb{P}$ denotes probability. By the Chernoff bound for a standard normal random variable

$$\begin{aligned} &\mathbb{P}\left(L_t\left(d, \mathbf{a}_{t-1}, \omega_{1,\ldots,t}\right) \leq Z_{t,d}|\omega_{1,\ldots,t}\right) \\ &\quad \leq \exp\left(-m\frac{{L_t}^2\left(d, \mathbf{a}_{t-1}, \omega_{1,\ldots,t}\right)}{2\sigma_t^2}\right). \end{aligned} \tag{16}$$

Using this bound and (12), the expected value of MTM throughput loss at each time slot is upper bounded by [26]

$$\begin{aligned} &\underset{\omega_{1,\ldots,t}}{\mathrm{E}} \left[L_t\left(d_{\mathrm{MTM}}, \mathbf{a}_{t-1}, \omega_{1\ldots,t}\right)\right] \\ &\quad = \sum L_t\left(d_{\mathrm{MTM}}, \mathbf{a}_{t-1}, \omega_{1\ldots,t}\right) \mathbb{P}\left(d_{\mathrm{MTM}}|\omega_{1,\ldots,t}\right) \\ &\quad \leq \sum L_t\left(d_{\mathrm{MTM}}, \mathbf{a}_{t-1}, \omega_{1\ldots,t}\right) \mathbb{P}(L_t\left(d, \mathbf{a}_{t-1}, \omega_{1,\ldots,t}\right) \\ &\quad \leq Z_{t,d}|\omega_{1,\ldots,t}) \\ &\quad \leq \sum L_t\left(d, \mathbf{a}_{t-1}, \omega_{1,\ldots,t}\right) \exp\left(-m\frac{L_t^2}{2\sigma_t^2}\right). \end{aligned} \tag{17}$$

In (6), the mean total throughput loss over all time slots for MTM scheduling is defined as the sum of throughput losses in each time slot. Therefore, the total throughput loss of MTM scheduling is upper bounded by taking the sum of the above-mentioned upper bound over all time slots.

Using the Chernoff bound, (17) shows that asymptotically, when m goes to infinity, in the limit, the upper bound for throughput loss goes to zero ([26, Th. 1]). In other words, by increasing the number of sets of samples m, the MTM scheduling accuracy increases and its performance approaches that of NRT scheduling with all CR demands revealed. However, increasing m implies more scheduling time. Hence, there is a tradeoff between accrued throughput and the portion of each time frame dedicated to scheduling. To this end, (17) gives the optimal number of sample sets for the CBS to keep the throughput loss of the CRN below a certain threshold.

The next section takes a deeper look into real-time scheduling for CRNs by considering the MTM and TLM algorithms within the context of MCDPs.

V. Real-Time CRN Scheduling Using Markov Chance Decision Processes

MCDP is an abstraction used to formulate real-time scheduling. An MCDP has the following components [27].

1) S is the finite set of states with $s_0 \in S$ as the initial state.
2) $(\xi_t)_{t\geq 0}$ is the input process. It is a time-homogeneous Markov chain on a state set I (the input states), specified by an initial distribution and a transition matrix.
3) $S \times I \to 2^S$ is the transition map.
4) $\mathscr{R} : S \times I \times S \to \mathbb{R}$ is the reward map.

As shown in Fig. 2, the radio environment map, i.e., the PU activities and status of the white spaces, such as spatial, temporal, or even angular resources [28], are modeled as a Markov chain $(\xi_t)_{t\geq 0}$, which evolves independently from the CRN but affects the CRN white space usage decisions. At each time t, the CR is in state s_t, observes the input i_t, which is a realization of ξ_t, and decides to transit to a new state s_{t+1}. An MCDP chain is a sequence of alternating states and observations denoted by

$$\mathscr{C} = s_0 \xrightarrow{i_0} s_1 \xrightarrow{i_1} \ldots. \tag{18}$$

The total CR throughput obtained by a chain $\mathscr{C}$, representing an MCDP sequence, is $\mathscr{R}(\mathscr{C})$, i.e., the sum of throughputs for all time slots $t \in 1, \ldots, \mathcal{T}$. Therefore, there is a throughput probability distribution associated with each chain of MCDP.

MCDPs and Markov decision processes are equivalent. It can be shown [27] why MCDPs are more efficient than Markov decision processes when modeling real-time CRN scheduling in which the orders of the CR demands are immaterial. The goal in Markov decision processes is to maximize the expected reward

$$\max_{\alpha_0} \underset{s_1}{\mathrm{E}} \left[\max_{\alpha_1} \mathrm{E}_{s_2} \left[\ldots \underset{s_\mathcal{T}}{\mathrm{E}} \left[\mathscr{R}\left(s_0 \xrightarrow{\alpha_0} s_1 \xrightarrow{\alpha_1} \cdots \xrightarrow{\alpha_{\mathcal{T}-1}} s_\mathcal{T}\right)\right]\right]\right]. \tag{19}$$

Here, $\mathscr{C}$ is the chain defined by the pair (α_t, s_{t+1}). Also, α_t is the action that causes the transition from state s_t to s_{t+1}. On the other side, in MCDPs, given state s_0 and observations i_0, compute

$$\max_{s_1} \underset{\xi_1}{\mathrm{E}} \left[\max_{s_2} \underset{\xi_2}{\mathrm{E}} \left[\ldots \underset{\xi_\mathcal{T}}{\mathrm{E}} \left[\mathscr{R}\left(s_0 \xrightarrow{i_0} s_1 \xrightarrow{\xi_1} \cdots \xrightarrow{\xi_{\mathcal{T}-1}} s_\mathcal{T}\right)\right]\right]\right]. \tag{20}$$

In (19) for Markov decision processes, state s_{t+1} depends on both s_t and α_t, whereas in (20) for Markov chance decision processes, the input process is exogenous, and ξ_{t+1} depends only on ξ_t, not on past decisions. Note that as in Fig. 2, i_t is a realization of the input process ξ_t, which is imposed on the CRN, as a result of the PU activity. To find the optimal CRN scheduling, the CBS has to compute

$$\max_{s_1} \mathop{\mathrm{E}}_{\xi_1}\left[\mathop{\mathrm{E}}_{\xi_2}\left[\dots \mathop{\mathrm{E}}_{\xi_{\mathcal{T}-1}}\left[\max_{s_2}\dots\max_{s_\mathcal{T}} \mathscr{R}\left(s_0 \overset{i_0}{\rightarrow} s_1 \cdots \overset{\xi_{\mathcal{T}-1}}{\rightarrow} s_\mathcal{T}\right)\right]\right]\right]. \tag{21}$$

To highlight the importance of using MCDP instead of Markov decision processes, note that (21) can be obtained by swapping E and $\max$ in (20) for Markov chance decision processes, but it cannot be derived from (19) in the same way. In other words, it is not possible to obtain (21) from (19) because the CRN has no control over PU activity ξ_t, in contrast to the actions α_t, which are modeled by Markov decision processes. This is one major benefit associated with MCDP, compared with the Markov decision process.

As mentioned, MCDP is a variation of Markov decision processes. In the Markov reward processes used in CRNs [29], the reward is determined by an unknown parameter. Clearly, the PU and CRN are two different networks, and it is challenging for the CRN to gain knowledge of the parameters of the PU channel activity stochastic process. In other words, when trying to learn about PU activity, within a Markov reward process context, the obstacle is to learn the underlying parameters that drive the stochastic process behind the PU activity. However, this paper, by using MCDPs, finds a way around this problem, so that without having to learn the PU channel activity, the objective of optimal CRN scheduling is achieved. More specifically, regardless of the underlying PU activity model, from the viewpoint of the CRN, PU activity is a realization i_t, which is an exogenous factor that causes the MCDP to change state.

To find optimal CRN schedules, the CBS has to compute the chain

$$\mathscr{C} = s_t \rightarrow s_{t+1} \rightarrow \cdots \overset{i_{\mathcal{T}-1}}{\rightarrow} s_\mathcal{T} \tag{22}$$

that maximizes the overall throughput. The maximization

$$\max_{s_2}\dots\max_{s_\mathcal{T}} \mathscr{R}\left(\mathscr{C}\right) \tag{23}$$

is a deterministic NRT optimization, since its premise is to assume that all unknown random variables $\xi_{1,\dots,\mathcal{T}-1}$ have been revealed. This NRT optimization problem returns a chain starting from state s_t with the input sequence $i_{t\dots\mathcal{T}-1}$ affecting the CR decision by originating from an external Markov chain, i.e., the PU white space usage activities. In view of this, (21) becomes

$$\max_{s_1} \mathop{\mathrm{E}}_{\xi_{1\dots\mathcal{T}-1}}\left[\mathscr{R}\left(s_0 \overset{i_0}{\rightarrow} \mathrm{NRT}\left(s_1, \xi_{1\dots\mathcal{T}}\right)\right)\right]. \tag{24}$$

If during the horizon $\mathcal{T}$ for scheduling, the order of CR decisions is not important in the overall CRN throughput, the real-time CRN scheduling

$$\mathop{\mathrm{E}}_{\xi_t}\left[\max_{s_{t+1}} \mathop{\mathrm{E}}_{\xi_{t+1}}\left[\dots\max_{s_\mathcal{T}} \mathscr{R}(s_t \overset{\xi_t}{\rightarrow} s_{t+1} \overset{\xi_{t+1}}{\rightarrow} \cdots \overset{\xi_{\mathcal{T}-1}}{\rightarrow} s_\mathcal{T})\right]\right] \tag{25}$$

can be approximated by

$$\mathop{\mathbb{E}}_{\xi_{t\dots\mathcal{T}-1}}\left[\mathscr{R}_{\mathrm{NRT}}\left(s_t, \xi_{t\dots\mathcal{T}-1}\right)\right]. \tag{26}$$

Algorithm 1: MTM-MCDP CRN Scheduling.

Input $i_0 \dots i_{\mathcal{T}-1}$
for $t \in 0 \dots \mathcal{T}-1$ **do**
  $\mathscr{R}(\breve{s}) \leftarrow \mathscr{R}\left(s_t, i_t, \breve{s}\right)$
  for $k \in 1, \dots, m$ **do**
    Take sample set $i^k_{t+1\dots\mathcal{T}-1}$
  end for
  $\mathscr{R}(\breve{s}) \leftarrow \mathscr{R}(\breve{s}) + \mathscr{R}_{\mathrm{NRT}}\left(\breve{s}, i^k_{t+1\dots,\mathcal{T}-1}\right)$
  $s_{t+1} = \arg\max_{\breve{s}} \frac{\mathscr{R}(\breve{s})}{m}$
end for

Algorithm 1 shows the MTM scheduling for CRN using Markov chance decision processes, to model the externally imposed white space usage by the PU.

At time t, the CBS must transit to a new white space usage state s_{t+1}, given the current state s_t and the revealed input i_t, associated with PU activity. To this end, the CBS uses m sets of samples and maintains a record of the throughputs of all possible decisions that result from migrating from s_t.

VI. Throughput Performance of CR Real-Time Scheduling Using Markov Chance Decision Processes

In this section, the throughput loss of MTM MCDP CRN scheduling is analyzed. The CRN MTM MCDP scheduling assumes that as long as the overall throughput is maximized, within a finite number of time slots, the order of CR white space scheduling demands is not important. In other words, the proposed CRN scheduling replaces the following real-time optimization:

$$\mathop{\mathrm{E}}_{\xi_{t+1}}\left[\max_{s_{t+2}} \mathop{\mathrm{E}}_{\xi_{t+2}}\left[\dots\max_{s_\mathcal{T}} \mathscr{R}\left(s_{t+1} \overset{\xi_{t+1}}{\rightarrow} s_{t+2} \overset{\xi_{t+2}}{\rightarrow} \cdots \overset{\xi_{\mathcal{T}-1}}{\rightarrow} s_\mathcal{T}\right)\right]\right] \tag{27}$$

with

$$\mathop{\mathrm{E}}_{\xi_{t+1,\dots\mathcal{T}-1}}\left[\mathscr{R}_{\mathrm{NRT}}\left(s_{t+1}, \xi_{t+1\dots\mathcal{T}-1}\right)\right]. \tag{28}$$

This may cause some throughput loss, which will be investigated in this section. The other cause of throughput loss may stem from replacing the expected value in (28) with the empirical averaging of samples

$$\frac{1}{m}\sum_{k=1}^{m} \mathscr{R}_{\mathrm{NRT}}\left(s_{t+1}, i^k_{t+1\dots\mathcal{T}-1}\right) \tag{29}$$

where $k \in 1, \dots, m$ and $i^k_{t+1,\dots,\mathcal{T}-1}$ is a sample set of random variables $\xi_{t+1,\dots,\mathcal{T}-1}$.

The following analysis shows how to calculate the expected throughput loss in each time slot t. By adding the expected throughput loss per time over all time slots $t \in \mathscr{T}$, the total throughput loss of the proposed CRN scheduling will be obtained.

The new white space usage state s^{MCDP}_t returned by MTM MCDP CRN scheduling is a random variable that is a function of the pair $(s^{\mathrm{MCDP}}_{t-1}, i_t)$ and the m sample sets. i_t is the realization of the random variable ξ_t and is the input dictated by the PU, revealed at time t. Also, s_{t-1} is the previous state of white space usage for the CRN. To formalize the throughput loss, note that the following two chains

$$\mathscr{C}_t = s_0^{\mathrm{MCDP}} \xrightarrow{i_0} \dots \xrightarrow{i_{t-2}} s_{t-1}^{\mathrm{MCDP}} \xrightarrow{i_{t-1}} \mathrm{NRT}\left(s_t^{\mathrm{MCDP}}, i_{t\dots\mathcal{T}-1}\right) \tag{30}$$

and

$$\mathscr{C} = s_0^{\mathrm{MCDP}} \xrightarrow{i_0} \dots \xrightarrow{i_{t-1}} s_t^{\mathrm{MCDP}} \dots \xrightarrow{i_{\mathcal{T}-1}} s_{\mathcal{T}}^{\mathrm{MCDP}} \tag{31}$$

are the same before reaching state s_t^{MCDP}. Also, $\mathscr{C} = \mathscr{C}_{\mathcal{T}}$. To determine the expected throughput loss per time slot, assume all decisions of the real-time scheduling by the CBS are the same as the NRT algorithm, except the channel scheduling at time t. The throughput loss per time slot of this CRN scheduling is

$$l_t = \mathscr{R}_{\mathrm{NRT}}\left(s_t, i_{t\dots\mathcal{T}-1}\right) - \mathscr{R}\left(s_t \xrightarrow{i_t} \mathrm{NRT}\left(s_{t+1}, i_{t+1\dots\mathcal{T}-1}\right)\right). \tag{32}$$

Here, $i_{t\dots\mathcal{T}-1}$ is a realization of random variables $\xi_{t\dots\mathcal{T}-1}$, obtained by sampling. The expected throughput loss per time slot of s_{t+1} is

$$\begin{aligned}\mathcal{L}_t\left(s_t, i_t, s_{t+1}\right) &= \mathcal{L}_{t1}\left(s_t, i_t\right) + \mathcal{L}_{t2}\left(s_t, i_t, s_{t+1}\right)\\ &= \mathop{\mathbb{E}}_{\xi_{t+1,\dots,\mathcal{T}-1}}\left[\mathscr{R}(\mathscr{C}_t) - \mathscr{R}(\mathscr{C}_{t+1})\right]\\ &= \mathbb{E}\Big[\mathscr{R}_{\mathrm{NRT}}\left(s_t, i_t : \xi_{t+1\dots\mathcal{T}-1}, s_{t+1}\right)\\ &\qquad - \mathscr{R}\left(s_t \xrightarrow{i_t} \mathrm{NRT}\left(s_{t+1}, \xi_{t+1\dots\mathcal{T}-1}\right)\right)\Big].\end{aligned} \tag{33}$$

This loss is due to having different sampling sets. For all sample sets representing the future, the overall MTM MCDP channel schedule by the CBS is s_{t+1}, whereas, due to averaging, for a single sample set, it may differ from s_{t+1}. This deviation causes throughput loss as

$$\begin{aligned}\mathcal{L}_{t1}(s_t, i_t) = &\mathop{\mathrm{E}}_{\xi_{t+1\dots\mathcal{T}-1}}\Big[\mathscr{R}\left(\mathrm{NRT}\left(s_t, i_t : \xi_{t+1\dots\mathcal{T}-1}\right)\right)\Big]\\ &- \underbrace{\max_{s_{t+1}^*} \mathop{\mathrm{E}}_{\xi_{t+1,\dots\mathcal{T}-1}}\Big[\mathscr{R}\big(s_t \to \mathrm{NRT}\big(s_{t+1}^*, \xi_{t+1\dots\mathcal{T}-1}\big)\big)\Big]}_{\text{replaced by empirical averaging}}.\end{aligned} \tag{34}$$

However, MTM scheduling returns s_{t+1} instead of the most optimal theoretical value of s_{t+1}^* in (34), due to calculating the empirical average using m sample sets instead of the second term in (34). This causes additional throughput loss, defined as

$$\begin{aligned}&\mathcal{L}_{t2}\left(s_t, i_t, s_{i+1}\right)\\ &= \max_{s_{t+1}^*} \mathop{\mathrm{E}}_{\xi_{t+1\dots\mathcal{T}-1}}\left[\mathscr{R}\left(s_t \xrightarrow{i_t} \mathrm{NRT}\left(s_{t+1}^*, \xi_{t+1\dots\mathcal{T}-1}\right)\right)\right]\\ &\quad - \max_{s_{t+1}^*} \mathop{\mathrm{E}}_{\xi_{t+1\dots\mathcal{T}-1}}\left[\mathscr{R}\left(s_t \xrightarrow{i_t} \mathrm{NRT}\left(s_{t+1}, \xi_{t+1\dots\mathcal{T}-1}\right)\right)\right].\end{aligned} \tag{35}$$

The MTM MCDP scheduling takes the empirical average of the total throughput for m sample sets $i_{t+1\dots\mathcal{T}-1}^1, \dots, i_{t+1\dots\mathcal{T}-1}^m$

$$\frac{1}{m}\sum_{k=1}^{m}\mathscr{R}\left(s \xrightarrow{i} \mathrm{NRT}\left(\breve{s}, \xi_{t+1\dots\mathcal{T}-1}^k\right)\right) \tag{36}$$

and returns a random variable s^{MCDP} corresponding to the new state of the CR white space usage, such that

$$s^{\mathrm{MCDP}} = \arg\max_{\breve{s}} \frac{1}{m}\sum_{k=1}^{m}\mathscr{R}\left(s \xrightarrow{i} \mathrm{NRT}\left(\breve{s}, \xi_{t+1\dots\mathcal{T}-1}^k\right)\right). \tag{37}$$

Consider a state s^* such that $\mathcal{L}_{t2}(s, i, s^*) = 0$. According to the definition of the throughput loss $\mathcal{L}_{t2}$ and the optimality of s^*

$$\begin{aligned}\mathcal{L}_{t2} = &\mathrm{E}\Big[\mathscr{R}(s \to \mathrm{NRT}(s^*, \xi_{t+1\dots\mathcal{T}-1}))\Big]\\ &- \mathrm{E}\Big[\mathscr{R}(s \to \mathrm{NRT}(\breve{s}, \xi_{t+1\dots\mathcal{T}-1}))\Big]\end{aligned} \tag{38}$$

When MTM selects the suboptimal state $\breve{s}$ instead of s^*, the selection must have been due to

$$\begin{aligned}&\frac{1}{m}\sum_{k=1}^{m}\mathscr{R}\left(s \xrightarrow{i} \mathrm{NRT}\left(\breve{s}, \xi_{t+1\dots\mathcal{T}-1}^k\right)\right)\\ &\quad \geq \frac{1}{m}\sum_{k=1}^{m}\mathscr{R}\left(s \xrightarrow{i} \mathrm{NRT}\left(s^*, \xi_{t+1\dots\mathcal{T}-1}^k\right)\right).\end{aligned} \tag{39}$$

Therefore, as shown in (40) at the bottom of this page, the throughput loss $\mathcal{L}_{t2}$ is equal to the term in (40) minus a positive value. Hence, it is upper bounded by Z in (40).

Additionally, the term

$$\begin{aligned}&\frac{1}{m}\sum_{k=1}^{m}\mathscr{R}\left(s \xrightarrow{i} \mathrm{NRT}\left(\breve{s}, \xi_{t+1\dots\mathcal{T}-1}^k\right)\right)\\ &\quad - \frac{1}{m}\sum_{k=1}^{m}\mathscr{R}\left(s^* \xrightarrow{i} \mathrm{NRT}\left(\breve{s}, \xi_{t+1\dots\mathcal{T}-1}^k\right)\right)\end{aligned} \tag{41}$$

$$\begin{aligned}Z = &\underbrace{\frac{1}{m}\sum_{k=1}^{m}\mathscr{R}\left(s \xrightarrow{i} \mathrm{NRT}\left(\breve{s}, \xi_{t+1\dots\mathcal{T}-1}^k\right)\right) - \frac{1}{m}\sum_{k=1}^{m}\mathscr{R}\left(s^* \xrightarrow{i} \mathrm{NRT}\left(\breve{s}, \xi_{t+1\dots\mathcal{T}-1}^k\right)\right)}_{\geq 0}\\ &\underbrace{- \mathop{\mathrm{E}}_{\xi_{t+1\dots\mathcal{T}-1}}\mathscr{R}\left(s \xrightarrow{i} \mathrm{NRT}\left(\breve{s}, \xi_{t+1\dots\mathcal{T}-1}\right)\right) + \mathop{\mathrm{E}}_{\xi_{t+1\dots\mathcal{T}-1}}\mathscr{R}\left(s \xrightarrow{i} \mathrm{NRT}\left(s^*, \xi_{t+1\dots\mathcal{T}-1}\right)\right)}_{\mathcal{L}_{t2}}\end{aligned} \tag{40}$$

in (40) is the average of m independent identically distributed random variables [27]. Denote the variance of each such random variable by σ^2. The expected value of each random variable is

$$\underset{\xi_{t+1\ldots\mathcal{T}-1}}{\mathrm{E}}\left[\mathscr{R}\left(s \rightarrow \mathrm{NRT}\left(\breve{s}, \xi_{t+1\ldots\mathcal{T}-1}\right)\right)\right] - \underset{\xi_{t+1\ldots\mathcal{T}-1}}{\mathrm{E}}\left[\mathscr{R}(s \rightarrow \mathrm{NRT}(s^{*}, \xi_{t+1,\ldots\mathcal{T}-1}))\right] \tag{42}$$

By the central limit theorem, $\frac{\sqrt{m}Z}{\sigma}$ has standard normal probability density function $\mathscr{N}(0,1)$. By definition of the expectation

$$\underset{s^{\mathrm{MCDP}}}{\mathrm{E}}\left[\mathcal{L}_{t2}\left(s,i,\breve{s}\right)\right] = \sum_{\breve{s}} \mathcal{L}_{t2}\left(s,i,\breve{s}\right)\mathbb{P}\left(s^{\mathrm{MCDP}} = \breve{s}\right). \tag{43}$$

As a result, the expected value of $\mathcal{L}_{t2}$ is upper bounded by

$$\begin{aligned}\underset{s^{\mathrm{MCDP}}}{\mathrm{E}}\left[\mathcal{L}_{t2}\right] &= \sum_{\breve{s}} \mathcal{L}_{t2}\left(s,i,\breve{s}\right)\mathbb{P}\left(s^{\mathrm{MCDP}} = \breve{s}\right)\\ &\overset{(a)}{\leq} \sum_{\breve{s}} \mathcal{L}_{t2}\left(s,i,\breve{s}\right)\mathbb{P}\left(\mathcal{L}_{t2}\left(s,i,\breve{s}\right) \leq Z\right)\\ &\overset{(b)}{\leq} \sum_{\breve{s}} \mathcal{L}_{t2}\left(s,i,\breve{s}\right)\exp\left(\frac{-m\mathcal{L}_{t2}\left(s,i,\breve{s}\right)^2}{2\sigma^2}\right)\end{aligned} \tag{44}$$

The inequality (a) results from $\mathcal{L}_2$ being upper bounded by Z, due to (39) and (40), i.e.,

$$\mathbb{P}\left(s^{\mathrm{MCDP}} = \breve{s}\right) \leq \mathbb{P}\left(\mathcal{L}_{t2}\left(s,i,\breve{s}\right) \leq Z\right). \tag{45}$$

Inequality (b) is a result of the Chernoff bound for the standard normal random variable

$$\mathbb{P}\left(\mathcal{L}_{t2}\left(s,i,\breve{s}\right) \leq Z\right) \leq \exp\left(\frac{-m\mathcal{L}_{t2}^2\left(s,i,\breve{s}\right)}{2\sigma^2}\right). \tag{46}$$

The next goal is to bound the total throughput loss. The expected value of the difference between $\mathscr{C}_0$, as defined by (30), and the chain in (31) is the total mean throughput loss of real-time MTM MCDP scheduling. This value is compared with the NRT delayed scheduling with perfectly known information over the horizon

$$\underset{\mathscr{C}}{\mathrm{E}}[\mathscr{R}(\mathscr{C}_0) - \mathscr{R}(\mathscr{C})] = \sum_{t=0}^{\mathcal{T}-1}\mathrm{E}\left[\mathcal{L}_t\left(s_t^{\mathrm{MCDP}}, \xi_t, s_{t+1}^{\mathrm{MCDP}}\right)\right] \tag{47}$$

The total throughput loss per time slot is the summation of $\mathcal{L}_{t1}$ and $\mathcal{L}_{t2}$. Hence,

$$\mathrm{E}\left[\mathcal{L}_t(s_t, \xi_t, s_{t+1}^{\mathrm{MCDP}})\right] = \mathrm{E}\left[\mathcal{L}_{t1}(s_t, i_t) + \mathcal{L}_{t2}\left(s_t, \xi_t, s_{t+1}^{\mathrm{MCDP}}\right)\right]. \tag{48}$$

Consider the case when

$$\mathcal{L}_{t1} \leq \epsilon \tag{49}$$

where $\mathcal{L}_{t1}\left(s_t, i_t\right)$ is defined in (34). Then

$$\mathrm{E}\left[\mathcal{L}_t(s_t, \xi_t, s_{t+1}^{\mathrm{MCDP}})\right] \leq \epsilon + \mathrm{E}\left[\mathcal{L}_{t2}(s_t, \xi_t, s_{t+1}^{\mathrm{MCDP}})\right]. \tag{50}$$

Using (44)

$$\mathrm{E}\left[\mathcal{L}_t\left(s_t, \xi_t, s_{t+1}^{\mathrm{MCDP}}\right)\right] \leq \epsilon + \underset{s_t,\xi_t}{\mathrm{E}}\left[\sum \mathcal{L}_{t2}\left(s_t, \xi_t, \breve{s}\right)\exp\left(\frac{-m\mathcal{L}_{t2}^2}{2\sigma^2}\right)\right] \tag{51}$$

and using (47)

$$\begin{aligned}&\underset{\mathscr{C}}{\mathrm{E}}\left[\mathscr{R}(\mathscr{C}_0) - \mathscr{R}(\mathscr{C})\right] \\ &= \sum_{t=0}^{\mathcal{T}-1}\mathrm{E}\left[\mathcal{L}_t\left(s_t, \omega_t, s_{t+1}\right)\right]\\ &\leq \sum_{t=0}^{\mathcal{T}-1}\left(\epsilon + \max_{s,i}\sum_{\breve{s}}\mathcal{L}_{t2}\left(s,i,\breve{s}\right)\exp\left(\frac{-m\mathcal{L}_{t2}\left(s,i,\breve{s}\right)^2}{2\sigma^2}\right)\right)\\ &\leq \mathcal{T}\left(\epsilon + \max\sum\mathcal{L}_{t2}\left(s,i,\breve{s}\right)\exp\left(\frac{-m\mathcal{L}_{t2}^2\left(s,i,\breve{s}\right)}{2\sigma^2}\right)\right).\end{aligned} \tag{52}$$

The aforementioned equation shows that there is an upper bound on the total throughput loss over all time slots of the deployed CRN scheduling method. Specially, by taking more samples, within the restricted scheduling time, the throughput performance can approach that of NRT scheduling, for which all information is already disclosed.

VII. Computational Complexity of MTM and TLM Schemes

Equation (17) provides insight into the complexity of MTM and TLM. When the number of samples in each step is $\Omega\left(\ln\left(\mathcal{T}|D|\right)\right)$, the expected value of the throughput loss of MTM will be $O\left(1\right)$ if the standard deviation σ_t of the throughput loss is $O\left(1\right)$. Here, Ω is the big-Ω notation for the asymptotic lower bound. Furthermore, since the total number of CR resource allocation demands is $|D|$ and since MTM considers each CR demand versus every sample set, $\Omega\left(\ln\left(\mathcal{T}|D|\right)\right)$ number of samples means the number of NRT calculations is $\Omega\left(|D|\ln\left(\mathcal{T}|D|\right)\right)$ [26]. As mentioned before, TLM is $|D|$ times faster than MTM because TLM does not consider every CR demand versus every set of samples. As such, TLM gives an approximation to the most optimal answer. To gain insight into how TLM performs in comparison with MTM, assume that TLM approximates the most optimal answer by a constant c. In other words, although the throughput of the NRT solution is higher than any approximation, the product of the approximated throughput $\widehat{\mathscr{R}}$ and the constant c becomes greater than the throughput of the NRT solution

$$c \geq \frac{\mathscr{R}_{\mathrm{NRT}}}{\widehat{\mathscr{R}}}. \tag{53}$$

Note that from (17), if the standard deviation σ_t of the throughput loss is $O\left(1\right)$, the difference between the expected approximated throughput of NRT scheduling and TLM scheduling is less than $O(1)$. This means that the expected throughput of the NRT solution is $1 + O\left(1\right)$ times the expected throughput of the

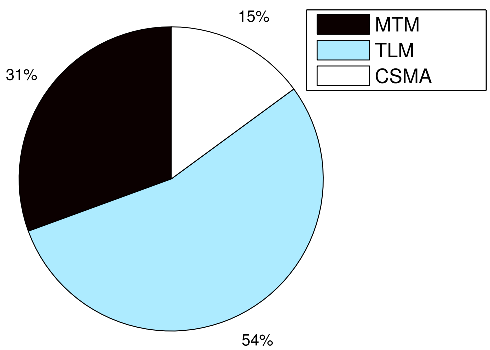

Fig. 3. Ratio of the average SNR ($\propto$ rate) of TLM scheduling, MTM, and CSMA.

TLM scheduling

$$\widehat{\mathscr{R}} = (1 + O(1))\, \mathscr{R}_{\text{TLM}}. \tag{54}$$

Multiplying both sides of (54) by c and inserting into (53) [26] gives

$$c\,(1 + O(1)) \geq \frac{\mathscr{R}_{\text{NRT}}}{\mathscr{R}_{\text{TLM}}}. \tag{55}$$

In other words, the ratio of the total throughput of the NRT scheduling (with perfect knowledge of all requests) to the throughput of the real-time TLM method is not more than $c\,(1 + O(1))$, which indicates acceptable performance of TLM.

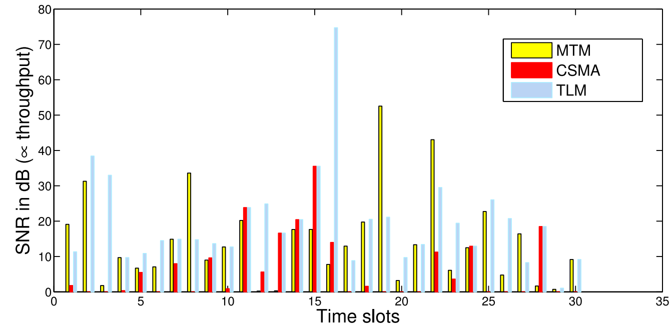

Fig. 4. SNR (proportional to rate) per time slot of the proposed TLM and MTM scheduling methods compared with that of CSMA.

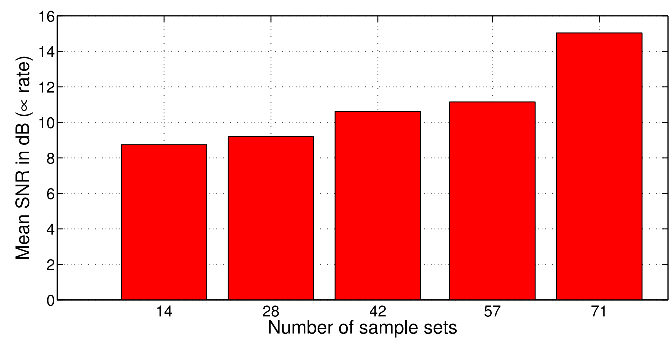

Fig. 5. SNR in dB ($\propto$ rate) averaged over all time slots versus the number of sample sets or time available to the CBS for scheduling decisions.

VIII. Numerical Evaluations

Simulations are performed in MATLAB for a number of CRs that contend over time slots. In each time slot, there are some CRs available to be scheduled. The demands of CRs for channel allocation are evaluated based on their SNRs, which are proportional to the data rate over the channel. At the beginning of each time slot, each CR n, $n \in \mathscr{N}$ is either handing off to a new channel or not, depending on the PU activity. More specifically, in each time slot, the PU either returns to the band or does not. The former causes the CR to evacuate and demand a new schedule. Therefore, without loss of generality, from the viewpoint of the CBS, at the beginning of each time frame, the scheduling demands of CRs can, for example, follow a Bernoulli distribution [14]–[17]. Furthermore, since Poisson distribution can represent arrivals within a time window, another viewpoint is to model the arrival and departure of users over a band as a Poisson process [29]. Assuming normalized noise over Rayleigh channels, the SNR of CR n over a channel originates from an exponential distribution. Accordingly, the CBS generates future demands of CRs by sampling. Then, for each sample, an exponential distribution is sampled to represent the SNR of a particular CR. The CBS selects the current demand that maximizes the objective function. SNRs of CRs are generated by samples of an exponential distribution with mean varying within the range of 5–20 dB. The CBS can, for instance, estimate the parameters for the distributions from statistics of previous observations. Fig. 3 shows the overall SNR (proportional to rate) ratio of MTM scheduling compared with CSMA over a horizon of 30 time slots for 12 CRs. At each time point, random numbers of CRs contend for the channel. This ratio is almost 54% to 31% to 15% for TLM, MTM, and CSMA, respectively. This ratio is obtained for the same scheduling time available to the CBS for both MTM and TLM methods.

Fig. 4 shows a comparison of SNR (proportional to the data rate) per time slot of the proposed TLM and MTM and CSMA. TLM is the method that yields higher rates considering the fairness constraint on CRs channel usage. The MTM method leads to the second best rate and CSMA comes last.

Fig. 5 shows the tradeoff between the speed of CBS in making a decision and the accuracy of the decision. There are a total of 12 CRs. In each time slot, some CRs contend for the channel. As the available time for the CBS to make a decision increases, the CBS can take more samples, and therefore, the accuracy of its scheduling increases. Accordingly, with increasing the number of sample sets, from 14 to 71 to make a scheduling decision in each time slot, the overall SNR (proportional to the rate) averaged over all time slots increases from approximately 9 to 15 dB. This result is in accordance with the upper bound derived in (17), which indicates that the throughput loss decreases as the number of samples increases.

Fig. 6 compares the speed of CBS while performing TLM and MTM channel allocation methods. As Fig. 6 shows, the slope of the number of samples versus scheduling time is greater for TLM than that of the MTM method. Using TLM, the CBS can take more number of sample sets into account than MTM during almost the same time interval. Accordingly, TLM is more accurate for finding the optimal CR. Fig. 7 compares TLM and

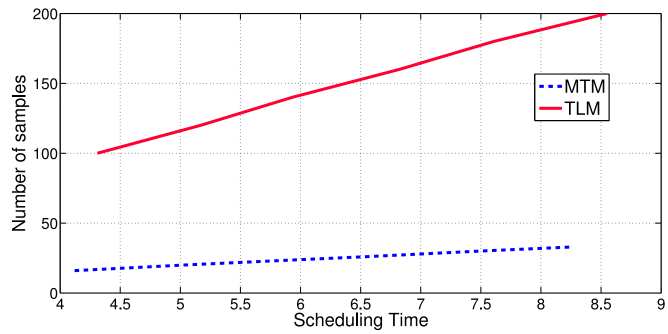

Fig. 6. Number of samples in MTM and TLM available to the CBS for a scheduling decision versus scheduling time

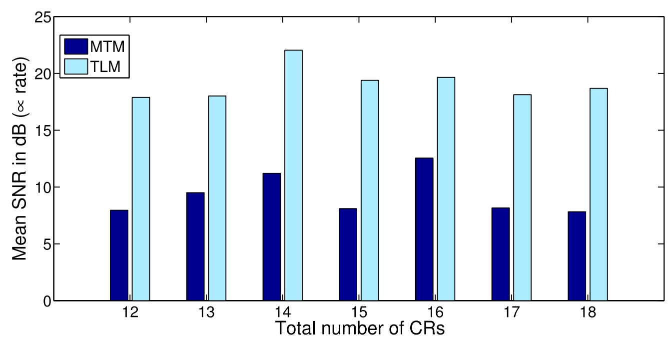

Fig. 7. Average SNR (∝ data rate) per time slot versus total number of CRs for TLM and MTM multiple access schemes.

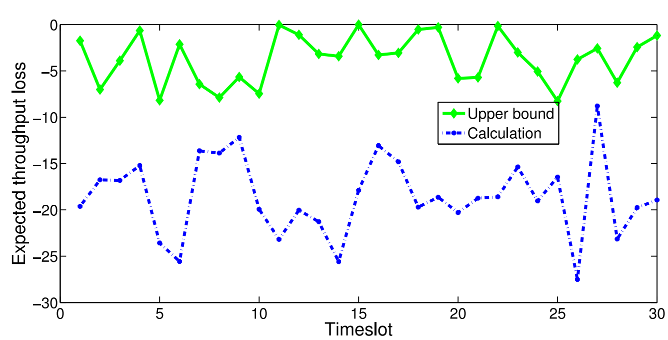

Fig. 8. Comparison of the calculated throughput loss per time slot for MTM with the upper bound of (17).

MTM in terms of the average SNR per time slot (proportional to the data rate) for TLM and MTM as the total number of CRs contending for spectrum holes in 30 time slots varies. The SNR of the CRs originates from an exponential probability density function with a mean of 10 dB. As Fig. 7 indicates, TLM yields higher rates than MTM by more optimal channel scheduling. Fig. 8 compares the throughput loss of MTM with the upper bound in (17).

Fig. 9 shows that the proposed scheduling methods outperform [19] in terms of overall rate. In [19], as long as a CR sends the spectrum sensing results, it is guaranteed to receive a channel, regardless of its SNR over that channel and fairness in scheduling. The reason is that the scheduling in [19] does not seek to select and schedule the CR with the maximum rate over a channel; rather it schedules CRs by their index. They assume the CRs are ordered in ascending order, based on CRs indices,

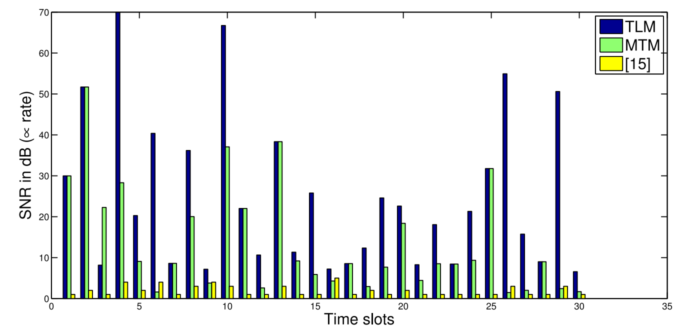

Fig. 9. Comparison of SNR (∝ rate) for MTM and TLM with the scheduling scheme presented in [19].

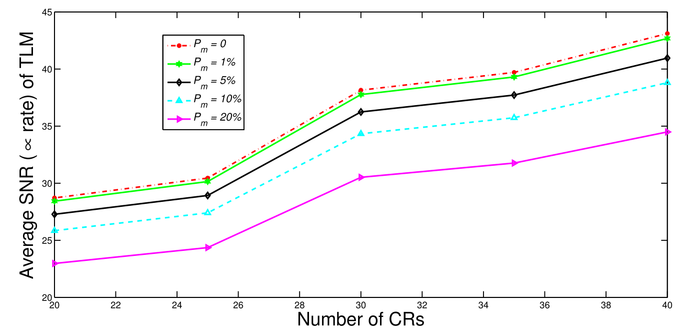

Fig. 10. Average SNR (∝ rate) for TLM versus the number of CRs for various probabilities of misdetection of PU (P_m)

and a CR with a lower index has priority for scheduling. In other words, if the index of a particular CR is lower, than CR can select a channel, even though the transmission of another CR might be of higher quality over that particular channel. Nevertheless, the advantage of the scheme presented in [19] is the dynamic selection of the common control channel.

Fig. 10 depicts the average performance of the CRN for various numbers of total CRs in the CRN, considering different probabilities of misdetecting PU activities. Higher probabilities of misdetection result in higher losses of CRN rate.

IX. Conclusion

Real-time multiple access schemes for CRNs are proposed in this paper. The schemes take into account short-lived idle primary channels and uncertainty about future primary and secondary users activities. The CBS allocates bands to CR user demands as they are revealed over time. To this end, the CBS makes optimal scheduling decisions based on past allocations, present demands, and samples that represent the future. The proposed methods are benchmarked by comparing the expected value of the sum throughput with that of NRT MAC.

In the proposed MTM scheduling, the goal of the CBS is to schedule a CR in each time slot to maximize the mean throughput over all time slots. To this end, the CBS evaluates each CR's present demand (SNR) against multiple sets of samples representing future demands. During the available scheduling time, and after evaluating the SNR (rate) for a number of sample sets, the CBS schedules the CR at time t with the highest evaluation score among all sample sets. The premise of the MTM CRN scheduling is to take samples of CRs scheduling demands in future time slots. In other words, from the viewpoint of the CBS, CRs scheduling demands of future time slots are random variables. Therefore, by taking samples from their probability distributions, the CBS transforms this scheduling problem, with incrementally revealed CR demands over time, into an NRT problem with known CR demands. This results in more accurate scheduling decisions. The CBS can take several sets of samples representing realizations of future CR demands. The CBS then calculates the overall throughput for each set of samples considering past scheduling decisions. The CBS schedules the CRs in present time slot t that maximize the expected value (mean) of throughput over all sample sets. When the number of CR demands is large or the available scheduling time is relatively short, the CBS switches to the TLM method for MAC. Using TLM, the CBS finds the optimal schedule by minimizing throughput loss. TLM estimates the throughput loss of a CR demand at time t using generated future sample sets. This allows TLM to be able to evaluate more sample sets than MTM within the available time. The CR with minimum total throughput loss over all generated sample sets receives the channel in TLM.

The tradeoffs between the available scheduling decision time and throughput loss are also discussed. The throughput losses of the proposed schemes are analyzed, and performance bounds are derived based on the number of sample sets or equivalently, the portion of each time slot dedicated to scheduling. The upper bound gives the optimal number of sample sets for the CBS to enhance the throughput of the CRN. As such, the CBS can keep the throughput loss below a certain level.

The efficiency of the proposed scheduling schemes is further verified by analyzing the computational complexity. In addition, it is demonstrated that although the proposed TLM scheduling is real time, its throughput performance is greater than a lower bounded fraction of the throughput obtained by ideal delayed NRT scheduling. Besides, Markov chance decision processes are used to model the radio environment map, i.e., PU activities and their effects on CR white space state transitions. Finally, upper bounds on throughput performance of CRNs are put forward using the Chernoff bound.

Acknowledgment

The author would like to thank the anonymous reviewers for their suggestions to improve the quality of this paper.

References

[1] F. Akhtar, M. H. Rehmani, and M. Reisslein, "White space: Definitional perspectives and their role in exploiting spectrum opportunities," *Telecommun. Policy*, vol. 40, pp. 319–331, Apr. 2016.

[2] T. Chen, H. Zhang, G. M. Maggio, and I. Chlamtac, "Topology management in CogMesh: A cluster-based cognitive radio mesh network," in *Proc. IEEE Int. Conf. Commun.*, 2007, pp. 6516–6521.

[3] J. J. Q. Zhang and X. S. Shen, "HC-MAC: A hardware-constrained cognitive MAC for efficient spectrum management," *IEEE J. Sel. Areas Commun.*, vol. 26, no. 1, pp. 106–117, Jan. 2008.

[4] V. K. Tumuluru, P. Wang, and D. Niyato, "A novel spectrum-scheduling scheme for multichannel cognitive radio network and performance analysis," *IEEE Trans. Veh. Technol.*, vol. 60, no. 4, pp. 1849–1858, May 2011.

[5] V. K. Tumuluru, P. Wang, D. Niyato, and W. Song, "Performance analysis of cognitive radio spectrum access with prioritized traffic," *IEEE Trans. Veh. Technol.*, vol. 61, no. 4, pp. 1895–1906, May 2012.

[6] M. Zheng, L. Chen, W. Liang, H. Yu, and J. Wu, "Energy-efficiency maximization for cooperative spectrum sensing in cognitive sensor networks," *IEEE Trans. Green Commun. Netw.*, vol. 1, no. 1, pp. 29–39, Mar. 2017.

[7] F. Han, S. Zhao, L. Zhang, and J. Wu, "Survey of strategies for switching off base stations in heterogeneous networks for greener 5G systems," *IEEE Access*, vol. 4, pp. 4959–4973, 2016.

[8] J. Wu, S. Guo, J. Li, and D. Zeng, "Big data meet green challenges: Greening big data," *IEEE Syst. J.*, vol. 10, no. 3, pp. 873–887, Sep. 2016.

[9] J. Wu, S. Guo, J. Li, and D. Zeng, "Big data meet green challenges: Big data toward green applications," *IEEE Syst. J.*, vol. 10, no. 3, pp. 888–900, Sep. 2016.

[10] X. Xing, T. Jing, W. Cheng, Y. Huo, and X. Cheng, "Spectrum prediction in cognitive radio networks," *IEEE Wireless Commun.*, vol. 20, no. 2, pp. 90–96, Apr. 2013.

[11] Y. Chen and H. S. Oh, "A survey of measurement-based spectrum occupancy modeling for cognitive radios," *IEEE Commun. Surv. Tutorials*, vol. 18, no. 1, pp. 848–859, Firstquarter 2016.

[12] M. Hyhty *et al.*, "Spectrum occupancy measurements: A survey and use of interference maps," *IEEE Commun. Surveys Tuts.*, vol. 18, no. 4, pp. 2386–2414, Fourthquarter 2016.

[13] Y. Saleem and M. H. Rehmani, "Primary radio user activity models for cognitive radio networks: A survey," *J. Netw. Comput. Appl.*, vol. 43, pp. 1–16, Aug. 2014.

[14] A. Ganti, E. Modiano, and J. N. Tsitsiklis, "Optimal transmission scheduling in symmetric communication models with intermittent connectivity," *IEEE Trans. Inf. Theory*, vol. 53, no. 3, pp. 998–1008, Mar. 2007.

[15] A. Banaei and C. N. Georghiades, "Throughput analysis of a randomized sensing scheme in cell-based ad-hoc cognitive networks," in *Proc. IEEE Int. Conf. Commun.*, Jun. 2009, pp. 1–6.

[16] J. Gambini, O. Simeone, Y. Bar-Ness, U. Spagnolini, and T. Yu, "Packet-wise vertical handover for unlicensed multi-standard spectrum access with cognitive radios," *IEEE Trans. Wireless Commun.*, vol. 7, no. 12, pp. 5172–5176, Dec. 2008.

[17] J. Gambini, O. Simeone, U. Spagnolini, Y. Bar-Ness, and Y. Kim, "Cognitive radio with secondary packet-by-packet vertical handover," in *Proc. IEEE Int. Conf. Commun.*, May 2008, pp. 1050–1054.

[18] A. C.-C. Hsu, D. S. L. Wei, and C.-C. J. Kuo, "A cognitive MAC protocol using statistical channel allocation for wireless ad-hoc networks," in *Proc. IEEE Wireless Commun. Netw. Conf.*, 2007, pp. 105–110.

[19] K. M. Thilina, E. Hossain, and D. I. Kim, "DCCC-MAC: A dynamic common control channel-based MAC protocol for cellular cognitive radio networks," *IEEE Trans. Veh. Technol.*, vol. 65, no. 5, pp. 3597–3613, May 2016.

[20] *IEEE Standard for Information Technology–Local and Metropolitan Area Networks, IEEE Std 802.22–2011*.

[21] M. Monemi, M. Rasti, and E. Hossain, "On characterization of feasible interference regions in cognitive radio networks," *IEEE Trans. Commun.*, vol. 64, no. 2, pp. 511–524, Feb. 2016.

[22] M. Monemi, M. Rasti, and E. Hossain, "Characterizing feasible interference region for underlay cognitive radio networks," in *Proc. IEEE Int. Conf. Commun.*, Jun. 2015, pp. 7603–7608.

[23] E. Biglier, A. Goldsmith, L. Greenstein, N. Mandayam, and H. V. Poor, *Principles of Cognitive Radio*. Cambridge, U.K.: Cambridge Univ. Press, 2012.

[24] E. Askari and S. Assa, "Full-duplex cognitive radio with packet fragmentation," in *Proc. IEEE Wireless Commun. Netw. Conf.*, Apr. 2014, pp. 1502–1507.

[25] H. Chang, R. Givan, and E. Chong, "Online scheduling via sampling," in *Proc. Artif. Intell. Plan. Scheduling*, 2000, pp. 62–71.

[26] P. V. Hentenryck, R. Bent, and E. Upfal, "Online stochastic optimization under time constraints," *Ann. Oper. Res.*, vol. 177, pp. 151–183, 2010.

[27] P. V. Hentenryck and R. Brent, *Online Stochastic Combinatorial Optimization*. Cambridge, MA, USA: MIT Press, 2009.

[28] S. Sodagari, "A secure radio environment map database to share spectrum," *IEEE J. Sel. Topics Signal Process.*, vol. 9, pp. 1298–1305, Oct. 2015.

[29] J. J. Alcaraz, M. Lopez-Martinez, J. Vales-Alonso, and J. Garcia-Haro, "Bandwidth reservation as a coexistence strategy in opportunistic spectrum access environments," *IEEE J. Sel. Areas Commun.*, vol. 32, no. 3, pp. 478–488, Mar. 2014.

Author's photograph and biography not available at the time of publication.